

Isotropic to Nematic Phase Transition in Carbon Nanotube dispersed Liquid Crystal Composites

Rajratan Basu, Krishna P. Sigdel and Germano S. Iannacchione*

Order-disorder phenomena laboratory, Department of Physics,
Worcester Polytechnic Institute, Worcester, Massachusetts 01609, USA

(Dated: October 11, 2018)

A high-resolution dielectric and calorimetric study of the isotropic (I) to nematic (N) phase transition of carbon nanotube (CNT) dispersed liquid crystal (LC) functional composites as a function of CNT concentration is reported. The evolution of the I - N phase transition, the temperature dependence of local nematic ordering formed by dispersed CNTs in the LC media and the transition enthalpy were coherently monitored. Anisotropic CNTs induce local deformation to the nematic director of LC and form lyotropic *pseudo-nematic* phase in the LC media. Results clearly indicate the dramatic impact of dispersed CNTs on both the isotropic and nematic phases of the composite.

PACS numbers: 64.70.mj, 81.07.De, 52.25.Mq, 65.40.Ba

Carbon nanotubes (CNTs) dispersed in a nematic liquid crystal (LC) represent a versatile functional composite that has gained interest in recent years for inducing parallel alignment of CNTs, improving electro-optic effect and switching behavior of LCs^{1,2,3,4,5,6}. The LC+CNTs system is a unique assemblage of an anisotropic dispersion (CNTs) in an anisotropic media (LC), which makes it an attractive physical system to study the phase transition phenomena. At the isotropic (I) to nematic (N) transition, the orientational order can be described by a symmetric and traceless second rank tensor (Q_{ij}) which can be described by a scalar parameter $S(T)$ on short length scale and on a longer length scale by a vector \hat{n} called nematic director⁷. In particular, orientational coupling of LC and MWCNTs has an impact on both the nematic and isotropic phases of LC as well as on I - N transition. These can be probed by studying the dielectric behavior of the composite. Dielectric constant of an anisotropic material like LC is orientation dependent. A nematic LC confined between parallel plate electrodes maintains a constant director, \hat{n} , due to plate boundary conditions. Planar LC molecules, being perpendicular to the probing field, show smallest dielectric constant, ε_{\perp} ; and homeotropically oriented (parallel to the probing field) LC molecules exhibit highest dielectric constant, ε_{\parallel} , assuming the LC is positive dielectric anisotropic. The dielectric anisotropy, $\Delta\varepsilon = (\varepsilon_{\parallel} - \varepsilon_{\perp})$, of LCs is one of the most important features to study their phase transitions. The average dielectric constant in a complete isotropic mixture is given by $\bar{\varepsilon} = (\varepsilon_{\parallel} + 2\varepsilon_{\perp})/3 = \varepsilon_{iso}$. In the uniaxial nematic phase the average dielectric constant can be written as $\bar{\varepsilon} = (a\varepsilon_{\parallel} + b\varepsilon_{\perp})$ which is lower than the extrapolated value of ε_{iso} . $\Delta\varepsilon$ depends on temperature and is proportional to the scalar order parameter, $S(T)$. Now, as the system reaches the complete disorder, *i.e.*, isotropic liquid, the order parameter drops down to zero. This leads to the idea of having no

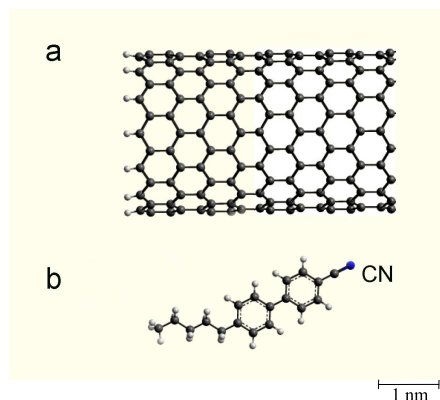


FIG. 1: Cartoons of **a)** one carbon nanotube structure, **b)** one 5CB liquid crystal molecule. The diagram of the MWCNT and 5CB are shown approximately to scale. Black spheres are carbon atoms and white spheres are hydrogen atoms.

temperature dependence of ε_{iso} .

In this paper, we present an experimental study of the nematic to isotropic phase transition in an LC+CNTs system for six different concentrations of multiwall carbon nanotubes (MWCNTs) in LC media, such as 0.05, 0.1, 0.15, 0.2, 0.25, and 0.3 wt %. Average dielectric constant ($\bar{\varepsilon}$) of such a system reveals information about local as well as long range nematic ordering. Calorimetric studies probe energy fluctuations of the phase transition character. Thus, a combined T -dependent dielectric and calorimetric investigation has been undertaken to study the I - N phase transition in LC+CNTs. This work reveals compelling evidence that nanotube aggregations create local and isolated short range orientation orders in the LC media which become prominent in the isotropic phase but does not cost any extra energy fluctuations for low CNT concentration.

*electronic address: gsiannac@wpi.edu

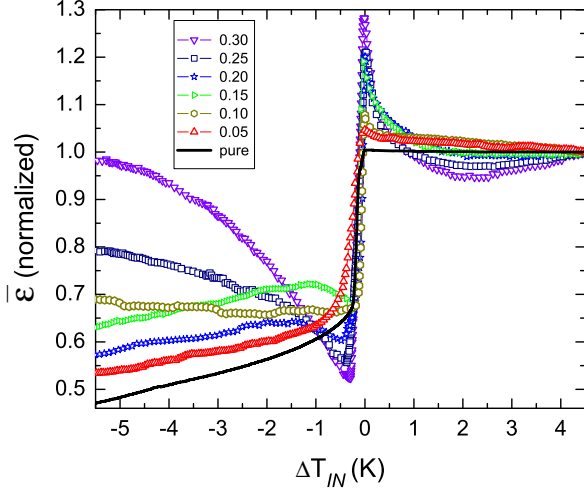


FIG. 2: Normalized average dielectric constant $\bar{\epsilon}$ for pure 5CB and 5CB+MWCNTs as a function of temperature shift, ΔT_{IN} . The legend shows the concentrations of dispersed MWCNTs in weight % in 5CB. The absolute values of T_{IN} for all concentrations are shown in Fig. 4a.

For these experiments, the well characterized liquid crystal 4-Cyano-4'-pentylbiphenyl (5CB) has been used as anisotropic host for MWCNTs. Pure 5CB (2 nm long and 0.5 nm wide, weakly polar molecule with $M = 249.359$ g/mol) has a weakly first-order isotropic to nematic phase transition at $T_{IN}^0 = 308$ K and strongly first order nematic to crystal transition at $T_{cr-N}^0 = 295.5$ K. Six different concentrations of MWCNT sample (containing nanotubes 5 - 30 nm in diameter and 1-5 μ m in length) in 5CB were prepared. After mixing each wt % of MWCNT sample with LC, the mixture was ultrasonicated for 5 hours. In general, nanotubes aggregate due to attractive mutual Van der Waals interactions but gentle ultrasonic agitations over a long period reduce tendency of bundling of nanotubes and effectively disperse and suspend them uniformly in a nematic LC matrix. Soon after ultrasonication, each mixture was degassed under vacuum at 40°C for at least two hours. In the LC+CNT system, helical surface anchoring of LC molecules to the CNT-wall enhances π - π stacking by maximizing the hexagon-hexagon interactions between this two species⁸. See Fig. 1. Due to these interactions, self-assembled LC molecules impose alignment on suspended carbon nanotubes along the nematic director^{1,2}.

AC capacitance bridge technique^{9,10,11} has been used to measure $\bar{\epsilon}$ as a function of temperature. A droplet of each mixture was sandwiched between parallel-plate capacitor configuration, 1 cm diameter and 100 μ m thick, housed in a temperature controlled bath. Dielectric measurements were performed at very low probing field (5kV/m) and at 100 kHz frequency. Comparison be-

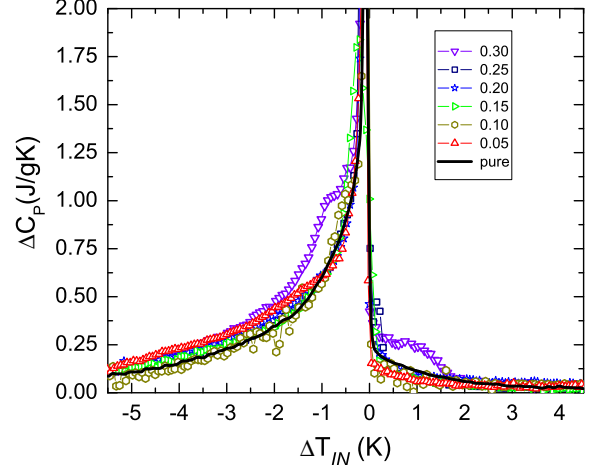


FIG. 3: Excess specific heat ΔC_p for pure 5CB and 5CB+MWCNTs as a function of temperature shift, ΔT_{IN} . The legend shows the concentrations of dispersed MWCNTs in weight % in 5CB. The absolute values of T_{IN} for all concentrations are shown in Fig. 4a.

tween the empty and sample filled capacitor allows for an absolute measurement of $\bar{\epsilon}(T)$. Since low probing field strength does not disturb the director orientation, no director reorientation occurred. The samples that were used in dielectric study were used in this AC calorimetry technique as well. The sample cell for calorimeter consists of an aluminum envelope of length ~ 15 mm, width ~ 8 mm and thickness ~ 0.5 mm with the three sides glued with super glue and was made using a cleaned sheet of aluminum. The aluminum was cleaned with water, ethanol and acetone using ultrasonic bath. Once the cell was dried thoroughly the desired amount of sample LC+CNTs was loaded into the cell and then a 120 Ω strain gauge heater and 1M Ω carbon-flake thermistor were attached on its surfaces. The filled cell then was mounted in the high resolution AC calorimeter^{12,13} to study the phase transition behavior. In the ac mode oscillating power $P_{ac} \exp(i\omega t)$ is applied to the cell resulting in the temperature oscillations with amplitude T_{ac} and a relative phase shift between T_{ac} and input power, $\varphi = \Phi + \frac{\pi}{2}$ where Φ is the absolute phase shift between T_{ac} and the input power. φ also provides the information regarding the order of the phase transition. With the definition of complex heat capacity, $C^* = \frac{P_{ac}}{\omega T_{ac}}$, the heat capacity at a heating frequency ω can be obtained^{14,15}. All calorimetric data presented here was taken at a heating frequency of 31.25 mHz at a scanning rate of 1 K h⁻¹. For all LC+CNTs samples each heating scan was followed by a cooling scan and experienced the same heating history.

The normalized $\bar{\epsilon}$ for different concentrations of LC+CNTs are shown in Fig. 2 as a function of tem-

perature shift ΔT_{IN} . The temperature shift is defined as $\Delta T_{IN} = T - T_{IN}$, where T_{IN} is the IN transition temperature for each concentration. The transition temperature is defined as the temperature where $\bar{\epsilon}$ shows the first discontinuity while entering the $N+I$ phase coexistence region from isotropic phase and was determined from $\bar{\epsilon}$ vs. T curves. Due to their high aspect ratio, CNTs also exhibit dielectric anisotropy and the value of average dielectric constant of aggregated CNTs is much larger than that of LCs¹⁶. The addition of a very tiny amount of MWCNT sample causes large increment in dielectric constant for the LC+CNTs composites. To compare the dielectric behaviors properly for all the concentrations, the dielectric constants are normalized to the highest temperature (315 K) point studied. Bulk 5CB exhibits the classic temperature dependence of the dielectric constant, showing nematic to isotropic phase transition at $T_{IN} = 308.1K$, seen in Fig. 2 and Fig. 4a. Above the transition temperature the dielectric constant flattens out in the isotropic phase and shows no temperature dependence at all ($\partial\epsilon_{iso}/\partial T \neq f(T)$), indicating that, bulk 5CB reaches complete disorder state having order parameter, $S(T) = 0$. $I-N$ phase transition for pure 5CB has been found at $T_{IN} = 307.8 K$ by using the AC calorimetry technique. The excess heat capacity, ΔC_p , associated with the phase transition can be determined by subtracting an appropriate background from total heat capacity over a wide temperature range^{14,17}. The resulting ΔC_p data for LC+CNTs samples studied are shown in Fig. 3 over a 10K temperature range window about ΔT_{IN} . The transition temperature is defined as the temperature of entering the $N+I$ phase coexistence region from isotropic phase and was determined from C_p'' vs. T curves. The excess heat capacity peaks are being shifted farther to zero of the temperature axis as the CNTs concentration increases, but the shifting does not have a fixed trend as also observed in dielectric results. The small shift on transition temperatures due to presence of CNTs is because of the large density differences between the liquid crystal and CNTs¹⁸. The $I-N$ transitions evolve in character. The nature of ΔC_p wings in Fig. 3 for $I-N$ transitions are the same for all samples. The highest concentration (0.3 wt %) studied shows two extra features at both sides of the transition. This is possibly due to the transition of *pseudo-nematic* phases⁶ of dispersed CNTs in LC media.

Different weight concentrations of the 5CB+MWCNTs functional composites reveal a dramatic change in the dielectric behavior as well as in nematic to isotropic phase transition behaviors. Smaller amount of CNTs dispersed and suspended in nematic LC media is not frozen in the system; rather they diffuse in the nematic matrix due to the thermal fluctuation. This can be visualized as annealed random variables evolving with time. The nano dynamics of CNTs induce local deformation of LC nematic director. The higher the CNT concentration the larger local deformation occurs. Dielectric behaviors also provide information about the molecular arrangements

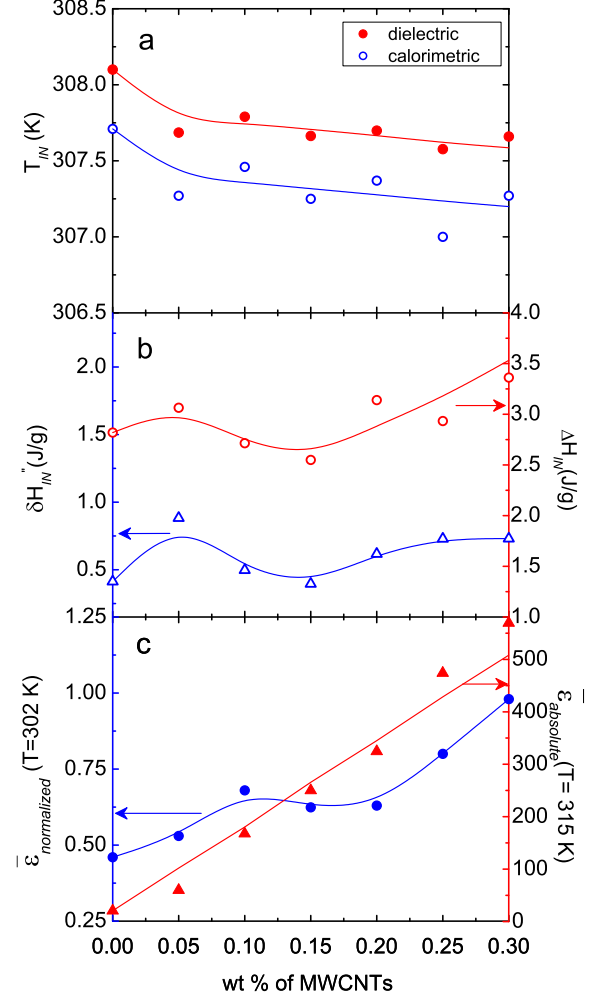


FIG. 4: **a)** The transition temperature, ΔT_{IN} , as a function of MWCNTs concentration and comparison between the two techniques used for the measurements, **b)** AC- enthalpy (right) and imaginary enthalpy (left) as a function of MWCNTs concentration, for details see text, **c)** The normalized dielectric constant, $\bar{\epsilon}$, as a function of MWCNTs concentration at the starting temperature, 302 K (left) and absolute dielectric constant in the deep isotropic phase (315 K) as a function of MWCNTs concentration (right).

in a particular system and the larger the $\Delta\epsilon$ the smaller electric field is needed to make an anisotropic system respond to it. $\Delta\epsilon$ of aggregated CNTs is much higher than that of LCs. $\Delta\epsilon$ increases locally in the LC+CNTs system in addition of CNTs. This makes the locally ordered domains, due to the presence of CNTs, more responsive to the probing field, hence the dramatic evolution in the nematic phase with different CNTs concentrations, clearly seen in Fig. 2. Fig. 4c shows the normalized $\bar{\epsilon}$ at the starting temperature (302 K) as a function of concentration of CNTs. Clearly there is a crossover region from 0.1 to 0.2 wt %. Above the crossover region the locally

ordered domains tend to align along the field and below that crossover region, the system is not that responsive to the low probing field. This explains the downward curvatures in the nematic phase for the higher concentrations observed in Fig. 2. Due to the elastic coupling and strong anchoring of LCs to nanotube-surfaces, both the species co-operatively create local short range orientation order. In addition to that, CNTs themselves form lyotropic nematic phase when they are dispersed in a fluid¹⁹. The curvatures in normalized $\bar{\epsilon}$ in the isotropic phase for LC+CNTs seen in Fig.2 are the evidence of presence of local *pseudo-nematic* order formed by CNTs in an isotropic liquid. The larger the CNT concentration the more curvature in $\bar{\epsilon}$ occurs above T_{IN} confirming that the formed local order is lyotropic *pseudo-nematic* phase. It has been observed that at about 315 K the $\bar{\epsilon}$ becomes independent of temperature for all concentrations, confirming that the thermal energy clears out the *pseudo-nematic* order and the system reaches complete isotropic state. The total enthalpy change associated with a first order phase transition is the sum of the pre-transitional enthalpy and latent heat. Due to partial phase conversion ($N \leftrightarrow I$) during a T_{ac} cycle, typical ΔC_p values obtained in two phase coexistence region are artificially high and frequency dependent. The procedure for calculating δH and ΔH is given in ref.¹⁴. An effective enthalpy change ΔH_{IN}^* which includes some of the latent heat contribution can be obtained by integrating observed ΔC_p peak. Here we performed a complete integration over the entire ΔC_p peak over a wide temperature range of around 300K to 312K for all 5CB+CNTs samples to get effective enthalpy change ΔH_{IN}^* associated with IN transition. The integration of the imaginary part of heat capacity gives imaginary enthalpy, $\delta H_{IN}''$, which indicates the first order character of the transition or the dispersion of energy in the sample. As fixed frequency used for this work $\delta H_{IN}''$ is only approximately proportional to the transition latent heat even though it is the measure of the dispersive part of the complex enthalpy. The proportionality constant is different for various CNT concentrations due to different values of the two phase conversion rate. The results of ΔH_{IN}^* and $\delta H_{IN}''$ as a function of CNT concentrations for all 5CB+CNTs samples are presented in Fig. 4b. Since ΔC_p values for the different concentration were different ac-enthalpy and imaginary enthalpy are also influenced by the CNT concentrations. ΔH_{IN}^* slightly increases with the increase in CNT concentration. The imaginary-enthalpy, $\delta H_{IN}''$ fluctuates slightly, but overall it also has the increasing trend with increase in CNT concentration. In ac-calorimetric technique the uncertainty in determining the enthalpy is typically 10%.

As demonstrated above, both dielectric and calorimetric measurements indicate that MWCNTs dispersed in 5CB create local lyotropic *pseudo-nematic* phase, but that does not change the net fluctuation of energy much during $I-N$ transition. Evolving wings of normalized $\bar{\epsilon}$ in the nematic phase in Fig. 2 indicate that local domains due to the presence of CNTs become more re-

sponsive to the probing field as CNT concentration increases in the system. A fixed trend in the curvature of $\bar{\epsilon}$ in isotropic phase with increasing CNT concentration manifests the para-nematic phase formed by dispersed CNTs in an isotropic fluid. Calorimetric study conspicuously evidences that tiny amount of suspended CNTs in LC does not cause considerable enthalpy fluctuation about the $I-N$ transition region. However, in the highest concentration (0.3 wt %), the *pseudo-nematic* phase formed by CNTs is strong enough and releases considerable amount of energy while melting, getting displayed in the ΔC_p vs. ΔT_{IN} graph. Additional electric field dependent experimental studies are planned to fully understand the character of field response of local domains in LC+CNTs system.

-
- ¹ M. D. Lynch and D. L. Patrick, Nano Letters **2**, 1197 (2002).
 - ² I. Dierking, G. Scalia, and P. Morales, J. Appl. Phys. **97**, 044309 (2005).
 - ³ I. Dierking, G. Scalia, P. Morales, and D. LeClere, Adv. Mater. **16**, 865 (2004).
 - ⁴ I.-S. Baik, S. Y. Jeon, S. H. Lee, K. A. Park, S. H. Jeong, K. H. An, and Y. H. Lee, Appl. Phys. Lett. **87**, 263110 (2005).
 - ⁵ P. V. Kamat, K. G. Thomas, S. Barazzouk, G. Girishkumar, K. Vinodgopal, and D. Meisel, J. Am. Chem. Soc. **126**, 10757 (2004).
 - ⁶ R. Basu and G. S. Iannacchione, Appl. Phys. Lett. **93**, 183105 (2008).
 - ⁷ P. G. de Gennes and J. Prost, *The Physics of Liquid Crystals* (Oxford University Press, Clarendon, Oxford, England, 1993).
 - ⁸ K. A. Park, S. M. Lee, S. H. Lee, and Y. H. Lee, J. Phys. Chem. C **111**, 1620 (2007).
 - ⁹ S. Pilla, J. A. Hamida, and N. S. Sullivan, Rev of Sci. Instrum. **70**, 4055 (1999).
 - ¹⁰ S. Bera and S. Chattopadhyay, Measurement **33**, 3 (2003).
 - ¹¹ M. C. Foote and A. C. Anderson, Rev of Sci. Instrum. **58**, 130 (1987).
 - ¹² P. F. Sullivan and G. Seidel, phys. Rev. **173**, 679 (1968).
 - ¹³ H. Yao and C. W. Garland, Rev. Sci. Instrum. **69**, 172 (1998).
 - ¹⁴ G. S. Iannacchione, C. W. Garland, J. T. mang, and T. P. Rieker, Phys. Rev. E **58**, 5966 (1998).
 - ¹⁵ A. Rosh, G. S. Iannacchione, P. Clegg, and R. J. Birge-neau, Phys. Rev. E **69**, 031703 (2004).
 - ¹⁶ R. Basu and G. Iannacchione, Appl. Phys. Lett. **92**, 052906 (2008).
 - ¹⁷ G. S. Iannacchione, Fluid Phase Equilibria **222/223**, 177 (2004).
 - ¹⁸ P. van der Schoot, V. Popa-Nita, and S. Kralj, J. Phys. Chem. B **112**, 4512 (2008).
 - ¹⁹ W. Song, I. A. Kinloch, and A. H. Windle, Science **302**, 1363 (2003).